*Journal of Global Positioning Systems (2007)*
*Vol.6, No.1: 13-22*

Journal of Global Positioning Systems
2007
© CPGPS

# Precise Point Positioning Using Combined GPS and GLONASS Observations

**Changsheng Cai, Yang Gao**

Department of Geomatics Engineering, University of Calgary, AB, Canada

**Abstract.** Precise Point Positioning (PPP) is currently based on the processing of only GPS observations. Its positioning accuracy, availability and reliability are very dependent on the number of visible satellites, which is often insufficient in the environments such as urban canyons, mountain and open-pit mines areas. Even in the open area where sufficient GPS satellites are available, the accuracy and reliability could still be affected by poor satellite geometry. One possible way to increase the satellite signal availability and positioning reliability is to integrate GPS and GLONASS observations. Since the International GLONASS Experiment (IGEX-98) and the follow-on GLONASS Service Pilot Project (IGLOS), the GLONASS precise orbit and clock data have become available. A combined GPS and GLONASS PPP could therefore be implemented using GPS and GLONASS precise orbits and clock data. In this research, the positioning model of PPP using both GPS and GLONASS observations is described. The performance of the combined GPS and GLONASS PPP is assessed using the IGS tracking network observation data and the currently available precise GLONASS orbit and clock data. The positioning accuracy and convergence time are compared between GPS-only and combined GPS/GLONASS processing. The results have indicated an improvement on the position convergence time but correlates to the satellite geometry improvement. The results also indicate an improvement on the positioning accuracy by integrating GLONASS observations.

**Keywords.** GPS, GLONASS, Precise Point Positioning, Precise orbit and Clock

## 1 Introduction

Current Precise Point Positioning (PPP) system developed is based on only GPS observations. The accuracy, availability and reliability of PPP positioning results however are quite dependent on the number of visible satellites. Under environments of urban canyons, mountains and open-pit mines, for instance, the number of visible GPS satellites is often insufficient for position determination (Tsujii, 2000). Further, even in the open area where sufficient GPS satellites are available, the PPP accuracy and reliability may still insufficient due to poor satellite geometry. One possible way to increase the availability of satellites as well as the reliability of the positioning results is to integrate GPS and GLONASS observations. The benefit from such integration is obvious particularly for applications in urban canyons, mountain and open-pit mining environments.

Since the International GLONASS Experiment (IGEX-98) and the follow-on GLONASS Service Pilot Project (IGLOS) conducted in 1998 and 2000 respectively (Weber, 2005), the precise GLONASS orbit and clock data have become available over times. Currently, four organizations can provide independent GLONASS precise orbits consistent at 10-15 cm level but only two centers provide post-mission GLONASS clock data (Oleynik, 2006). This provides opportunities to use GLONASS observations to improve precise point positioning accuracy and reliability currently based on only GPS observations. Although GLONASS achieved its Full Operational Capability (FOC) in January 1996 when 24 GLONASS satellites were available for positioning and timing, its constellation had dropped to several satellites by the year of 2001 due to a decrease in GLONASS budget (Zinoviev, 2005). As of Nov. 19, 2007, there are 18 GLONASS satellites in orbit but only 9 of them are operational satellites. However, the Russian government has approved a long-term plan to reconstitute a GLONASS constellation of 24 satellites. 18 satellites are expected to be operational by 2008, and a full operational capability with 24 satellites will be achieved

by 2010-2011. By that time, the number of GLONASS satellites will not be a problem any more.

In this paper, we will investigate the integration of GPS and GLONASS observations for improved accuracy and reliability of positioning results using PPP. The quality and characteristics of currently available precise GLONASS orbit and clock products are first described. The positioning model for combined processing of GPS and GLONASS observations is then presented. IGS tracking network observation data and available precise GLONASS orbit and clock data are used to assess the performance of combined GPS and GLONASS precise point positioning. Comparisons are also conducted on the numerical results between GPS only and combined GPS/GLONASS processing.

## 2 GLONASS Precise Orbit and Clock Products

GLONASS has been on the way to its modernization. In 2003, the first GLONASS-M satellite was launched, where "M" stands for Modified. On December 25, 2006, three GLONASS-M satellites (GLONASS 715, GLONASS 716 and GLONASS 717) were launched. All the three satellites are placed on orbit II. The GLONASS-M is a modernized version of the GLONASS spacecraft which supports a number of new features, such as the satellite design-lifetime increased to 7 years, a second civil modulation on L2 signal, and improved clock stability. The third generation GLONASS satellite "GLONASS-K" is expected to launch in 2008. The satellite service life is further increased to 10-12 years and a third civil signal frequency and Synthetic Aperture Radar function will be added (Sergey, 2007). The GLONASS-K represents a radical change in GLONASS spacecraft design, adopting a non pressured and modular spacecraft bus design (Kaplan, 2006).

The International GLONASS Experiment (IGEX-98) is the first global GLONASS observation and analysis campaign for geodetic and geodynamics applications, conducted from October 19, 1998 to April 19, 1999 and organized jointly by the International GNSS Service (IGS), the International Association of Geodesy (IAG) and the International Earth Rotation Service (IERS). The main objectives of the experiment were to collect a globally-distributed GLONASS dataset by using dual-frequency GLONASS receivers and determine the precise GLONASS satellite orbit. IGEX-98 has a global network consisting of 52 stations with 19 dual-frequency and 13 single-frequency receivers. For the IGEX-98 campaign, an infrastructure comparable to that of the IGS was established (Habrich, 1999). IGEX-98 includes the production of precise orbits for all the operational GLONASS satellites (Weber, 2005).

The International GLONASS Service Pilot Project (IGLOS) is a follow-on project of IGEX-98 that began in 2000 with the major purpose to integrate the GLONASS satellite system into the operation of IGS. The IGLOS Pilot Project has a global network consisting of about 50 tracking stations with dual-frequency GLONASS receivers. The GLONASS data are collected continuously and archived in RINEX format at the IGS Global Data Centers (Weber, 2005). The GPS and GLONASS observations are processed simultaneously and therefore the precise orbit products for both systems are given in one unique reference frame (Weber, 2002).

Currently four IGS analysis centers are routinely providing GLONASS precise orbit products. They are CODE (University Berne, Switzerland), IAC (Information - Analytical Center), ESA/ESOC (European Space Operations Center, Germany) and BKG (Bundesamt für Kartographie und Geodäsie, Germany).

CODE can generate the final GLONASS orbit as well as the rapid and predicted rapid orbit products (Weber, 2005; Schaer, 2004). The CODE orbits are expressed in the IGb00 reference frame, which is the IGS realization of the ITRF2000 (Bruyninx, 2007). IAC is a department at MCC (Russian Mission Control Center) which is routinely monitoring the GLONASS performance. Starting from 2004, IAC started to conduct routine orbit and clock determination based on IGS tracking network data. Since 2005 IAC has become one of the four IGS analysis centers who are routinely providing GLONASS post-mission orbit and clock data including (Oleynik,2006):

a) the final orbit and clock data with a delay of 5 days;
b) the rapid orbit and clock data with a delay of 1 day.

ESA/ESOC began to process and analyze GNSS data for precise orbit determination in 1991, first using its GPSOBS/BAHN software to compute the precise GPS orbits and clock parameters and then aligning its GLONASS solution to the ITRF2000 reference frame using the GPS orbits and tight constrains on the coordinates of 7 observing stations (Romero, 2004).

BKG has processed and analyzed the combined GPS/GLONASS observations from a network of global tracking stations since the beginning of the IGEX-98. Similar to ESA/ESOC, BKG first computes GPS orbits, clock estimation and earth orientation parameters and then utilizes the Bernese software to produce precise GLONASS orbits and station coordinates on a daily basis using double-differenced phase observations (Habrich, 2004). It provides GLONASS precise orbits, receiver-specific estimates of the system time difference between GPS and GLONASS, and the station coordinates (SINEX files).

The independent GLONASS orbits from the above four organizations are consistent at the 10-15cm level and have been combined to generate the IGS final GLONASS orbits using a procedure similar to IGS final GPS orbit (Weber, 2005).

As to precise satellite clock data, currently only two data analysis centers, namely IAC and ESA/ESOC, provide post-mission GLONASS clock data. The direct comparison of precise colock data from different centers however can hardly be conducted due to different reference time scales used and different inter-frequency biases applied to the GLONASS code measurements. The agreement between the IAC and ESOC post-mission GLONASS clock values is considered at the level of 1.5ns (Oleynik, 2006).

## 3 Combined GPS/GLONASS Data Processing for PPP

In the following, the positioning model for a combined GPS and GLONASS PPP system is described along with mathematical equations.

Based on a dual-frequency GPS/GLONASS receiver, the pseudorange and carrier phase observables on L1 and L2 between a receiver and a satellite can be described by the following observation equations:

$$P_i^g = \rho_g + cdt^g - cdT^g + d_{orb}^g + d_{trop}^g + d_{ion/P_i}^g + d_{mult/P_i}^g + \varepsilon_{P_i}^g \quad (1)$$

$$\Phi_i^g = \rho_g + cdt^g - cdT^g + d_{orb}^g + d_{trop}^g - d_{ion/\Phi_i}^g + \lambda_i^g N_i^g + d_{mult/\Phi_i}^g + \varepsilon_{\Phi_i}^g \quad (2)$$

$$P_i^r = \rho_r + cdt^r - cdT^r + d_{orb}^r + d_{trop}^r + d_{ion/P_i}^r + d_{mult/P_i}^r + \varepsilon_{P_i}^r \quad (3)$$

$$\Phi_i^r = \rho_r + cdt^r - cdT^r + d_{orb}^r + d_{trop}^r - d_{ion/\Phi_i}^r + \lambda_i^r N_i^r + d_{mult/\Phi_i}^r + \varepsilon_{\Phi_i}^r \quad (4)$$

where the superscript $g$ and r refer a GPS and a GLONASS satellite respectively, and

$P_i$ is the measured pseudorange on $L_i$ (m);
$\Phi_i$ is the measured carrier phase on $L_i$ (m);
$\rho$ is the true geometric range (m);
$c$ is the speed of light (m/s);
$dt$ is the receiver clock error (s);
$dT$ is the satellite clock error (s);
$d_{orb}$ is the satellite orbit error (m);
$d_{trop}$ is the tropospheric delay (m);
$d_{ion/L_i}$ is the ionospheric delay on $L_i$ (m);
$\lambda_i$ is the wavelength on $L_i$ (m/cycle);
$N_i$ is the integer phase ambiguity on $L_i$ (cycle);
$d_{mult/P_i}$ is the multipath effect in the measured pseudorange on $L_i$ (m);
$d_{mult/\Phi_i}$ is the multipath effect in the measured carrier phase on $L_i$ (m);
$\varepsilon$ is the measurement noise (m);

A system time difference unknown parameter should be introduced for mixed GPS/GLONASS observation processing (Habrich, 1999). A receiver clock error can be described as

$$dt = t - t_{sys} \quad (5)$$

where $t_{sys}$ denotes either GPS system time $t_{GPS}$ for GPS observations or GLONASS system time $t_{GLONASS}$ for GLONASS observations. Since the receiver clock error is related to a system time, the combined GPS and GLONASS processing includes two receiver clock offset unknown parameters, one for the receiver clock offset with respect to the GPS time and one for the receiver clock offset with respect to the GLONASS time. We can also describe the GLONASS receiver clock offset as follows:

$$\begin{aligned} dt^r &= t - t_{GLONASS} \\ &= t - t_{GPS} + t_{GPS} - t_{GLONASS} \\ &= dt^g + dt_{sys} \end{aligned} \quad (6)$$

which is a function of the GPS receiver clock offset and a system time difference between GPS and GLONASS. Applying equation (6) into equations (3) and (4) results in the following pseudorange and carrier phase observation equations:

$$P_i^r = \rho_r + cdt^g + cdt_{sys} - cdT^r + d_{orb}^r + d_{trop}^r + d_{ion/P_i}^r + d_{mult/P_i}^r + \varepsilon_{P_i}^r \quad (7)$$

$$\Phi_i^r = \rho_r + cdt^g + cdt_{sys} - cdT^r + d_{orb}^r + d_{trop}^r - d_{ion/\Phi_i}^r + \lambda_i^r N_i^r + d_{mult/\Phi_i}^r + \varepsilon_{\Phi_i}^r \quad (8)$$

Before GPS and GLONASS observations are used for position determination, the GPS and GLONASS precise orbit and clock data should be first applied to correct satellite orbit errors and satellite clock offsets. The ionospheric refraction bias can be eliminated by constructing an ionosphere-free combination of phase or pseudorange observable from the L1 and L2 frequencies. After the application of precise orbit and clock

corrections, the ionosphere-free code and phase combinations can be written as follows:

$$P_{IF}^{g} = (f_{g1}^{2} \cdot P_{1}^{g} - f_{g2}^{2} \cdot P_{2}^{g}) / (f_{g1}^{2} - f_{g2}^{2}) = \rho_{g} + cdt^{g} + d_{trop}^{g} + \varepsilon_{P_{IF}}^{g} \quad (9)$$

$$\Phi_{IF}^{g} = (f_{g1}^{2} \cdot \Phi_{1}^{g} - f_{g2}^{2} \cdot \Phi_{2}^{g}) / (f_{g1}^{2} - f_{g2}^{2}) = \rho_{g} + cdt^{g} + d_{trop}^{g} + N_{IF}^{g} + \varepsilon_{\Phi_{IF}}^{g} \quad (10)$$

$$P_{IF}^{r} = (f_{r1}^{2} \cdot P_{1}^{r} - f_{r2}^{2} \cdot P_{2}^{r}) / (f_{r1}^{2} - f_{r2}^{2}) = \rho_{r} + cdt^{g} + cdt_{sys} + d_{trop}^{r} + \varepsilon_{P_{IF}}^{r} \quad (11)$$

$$\Phi_{IF}^{r} = (f_{r1}^{2} \cdot \Phi_{1}^{r} - f_{r2}^{2} \cdot \Phi_{2}^{r}) / (f_{r1}^{2} - f_{r2}^{2}) = \rho_{r} + cdt^{g} + cdt_{sys} + d_{trop}^{r} + N_{IF}^{r} + \varepsilon_{\Phi_{IF}}^{r} \quad (12)$$

where

$P_{IF}$ is the ionosphere-free code combination (m);
$\Phi_{IF}$ is the ionosphere-free phase combination (m);
$f_i$ is the frequency of $L_i$ (Hz);
$N_{IF}$ is the combined ambiguity term (m);
$\varepsilon_{IF}$ contains measurement noise, multipath as well as other residual errors.

The unknown parameters of the positioning model based on the above observation equations include three position coordinates, a receiver clock offset, a system time difference, a zenith wet tropospheric delay, and ambiguity parameters equal to the number of observed GPS and GLONASS satellites. The dry tropospheric delay error is first corrected using the Hopfield tropospheric model and the remained zenith wet tropospheric delay (ZWD) including the residual dry delay is to be estimated as an unknown parameter. The Niell Mapping Functions have been used for hydrostatic and wet mapping functions. The positions, clock offset, system time difference and ZWD are modeled as a random walk process while the ambiguity parameters are modeled as constants and are to be estimated using a Kalman filter.

The basic procedure of PPP processing based on combined GPS and GLONASS observations is demonstrated in Fig. 1.

## 4 Numerical Results and Analysis

To assess the obtainable positioning accuracy based on combined GPS and GLONASS observations, numerical computations are conducted and the obtained results are presented in this section. At first, the PPP processing results including the positioning error, the receiver clock offset, the zenith wet tropospheric delay and the system time difference are given. Then comparisons are conducted to assess the positioning accuracy and the convergence time. Slow position convergence time is currently an obstacle for PPP applications and the additional observations from GLONASS are expected to reduce the required convergence time.

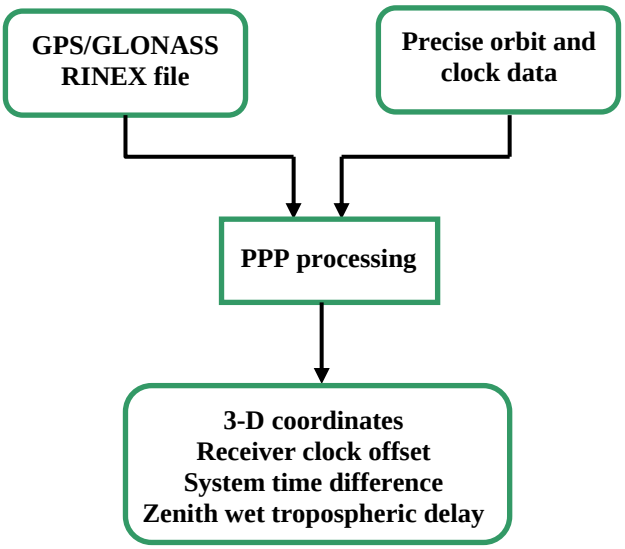


Fig. 1 PPP processing for combined GPS and GLONASS

### Data Descriptions

GPS/GLONASS observation datasets, collected on April 26th, 2007 at the IGS station HERT, GOPE and YARR, were downloaded from the IGS website. Each station was installed with an ASHTECH Z18 dual-frequency GPS/GLONASS receiver. Data sampling rate was 30s. The mixed GPS/GLONASS precise satellite orbit and 5-minute clock data generated by IAC data analysis center were downloaded from the IAC website. A total of 12 GLONASS satellites were operational on that day.

### Positioning Results

Twelve hours of observations acquired at the station HERT from EPN (EUREF Permanent Network) Local Analysis Centers were first used. The elevation mask was set to 10 degrees. The GPS only and the GPS/GLONASS observations were processed respectively. Fig. 2 shows the position errors over the period. It can be clearly observed that the positioning errors for GPS only and combined GPS/GLONASS processing are at a quite similar level.

Table 1 shows the mean, RMS, and standard deviation (one-sigma) of the converged position errors based on the results from local time 3:00 to 12:00. The differences in the mean, RMS and STD values for all three coordinate components are less than 1.5 cm.

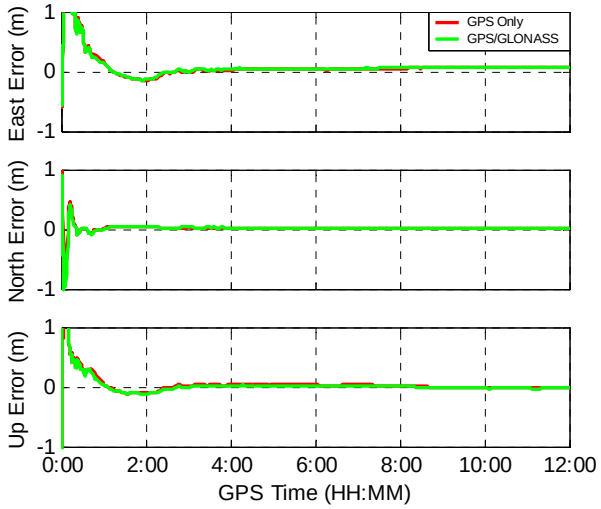


Fig. 2 GPS only vs. GPS/GLONASS positioning errors

Tab. 1 Statistics of Position Results (m)

| | | GPS Only | GPS / GLONASS |
|---|---|---|---|
| MEAN | East | 0.045 | 0.057 |
| | North | 0.012 | 0.016 |
| | Up | 0.012 | 0.001 |
| STD | East | 0.016 | 0.014 |
| | North | 0.006 | 0.006 |
| | Up | 0.020 | 0.020 |
| RMS | East | 0.048 | 0.058 |
| | North | 0.014 | 0.017 |
| | Up | 0.024 | 0.020 |

In addition to position determination, PPP can also output receiver clock offset solution which has the potential to support precise time transfer applications. The estimated receiver clock offsets in both GPS only and GPS/GLONASS processing are presented in Fig. 3. The red curve stands for the results from GPS only processing, which is completely overlapped by the green curve from the GPS/GLONASS processing results. Since the clock offset difference, which has a RMS value of 0.01 ns, is very small, the addition of GLONASS observations did not have a significant impact on the estimation of the receiver clock.

Presented in Fig. 4 is the estimated zenith wet tropospheric delay. As can be seen, the ZWD difference between the GPS only processing and the combined GPS/GLONASS processing after the position convergence is not significant with a RMS value of 2 mm.

The estimated system time difference is presented in Fig. 5. The system time difference varies in a range of about 4 ns over the twelve hours, which partially reflects the accuracy of the GLONASS system time scale. The greater variation before the GPS time 2:00 is due to the position convergence process. The obtained system time difference from the combined GPS/GLONASS data processing in PPP includes not only the time difference between the GPS and GLONASS system times but also the receiver hardware delay differences between GPS and GLONASS. Since they can not be separated from each other, the obtained value is the combined system time difference and receiver's inter-system hardware delay. As a result, the estimated system time difference should be considered as only an approximation to the true system time difference and is quite dependent on the receiver used.

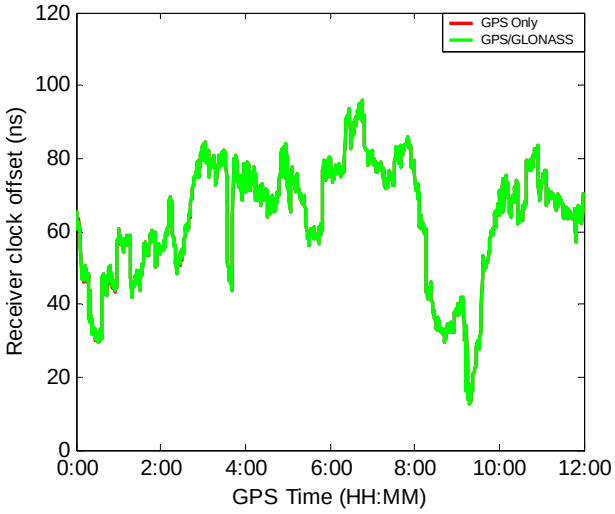


Fig. 3 GPS only vs. GPS/GLONASS receiver clock offset estimates

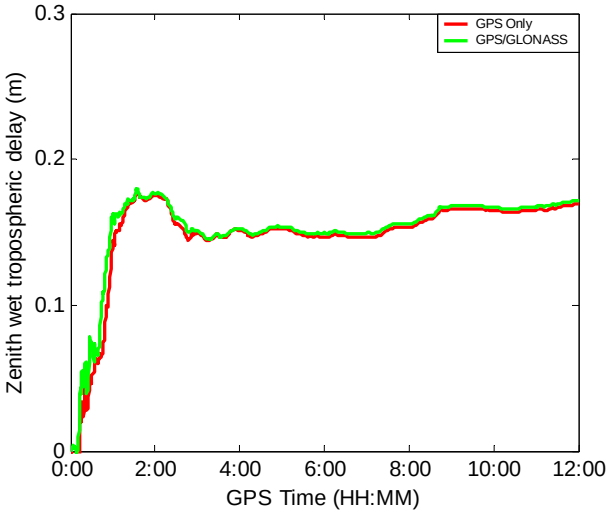


Fig. 4 GPS only vs. GPS/GLONASS zenith wet tropospheric delay estimates

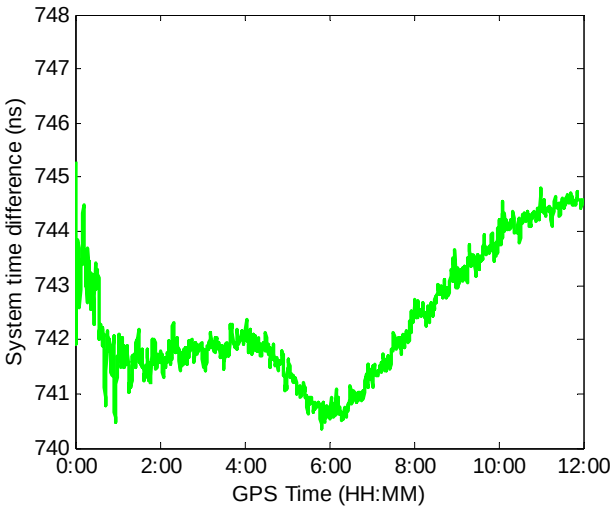


Fig. 5 Estimated system time differences

**Positioning Accuracy and Convergence Analysis**

Four processing sessions, each with three-hour data from three IGS stations, namely HERT, GOPE and YARR, were included in the data analysis. The elevation masks were set to 10 degrees. For each session, in addition to the position errors, the PDOP value and the number of used satellites were also calculated. The computation of the PDOP values in GPS/GLONASS processing is based on the design matrix corresponding to the unknowns of the three position coordinates, the receiver clock offset and the system time difference. This design matrix has one more column compared to the design matrix used for PDOP computation in the GPS only processing. The processing results are presented in Figs. 6-17.

Fig. 6 shows the positioning results between 0:00 and 3:00 at HERT station. No significant PDOP improvement is found before the position solutions converge and as a result, no significant convergence improvement is found. Presented in Fig. 7 are the processing results from the GPS time 3:00 to 6:00. In this session, two GLONASS satellites were utilized on average. Although in the beginning the PDOP value has only a slight improvement by adding GLONASS observations, the convergence time has been reduced significantly in the east and up directions.

In Fig.e 8, although PDOP has a significant improvement from the local time 6:42 to 7:02, no significant convergence improvement is found. This is because such a geometry improvement with more visible satellites was present after the position solutions have already converged. Looking at the results in Fig. 9, the PDOP improvement occurred at the first half an hour and during the convergence process. As a result, it has reduced significantly the position convergence time for horizontal coordinate components.

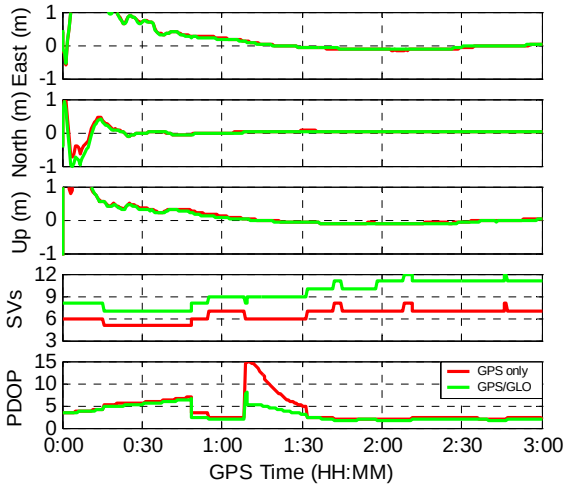


Fig. 6 Processing results at HERT (Session 1)

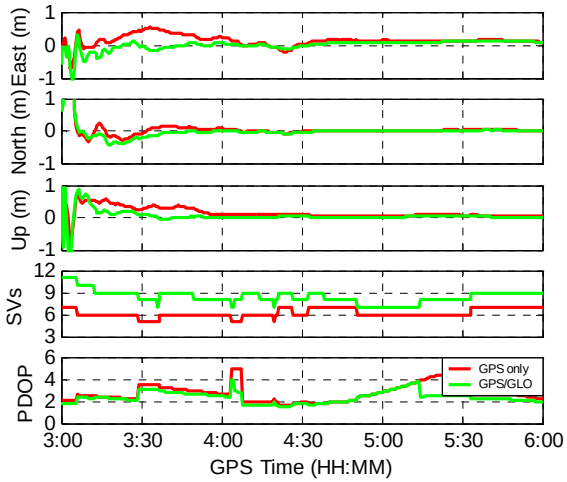


Fig. 7 Processing results at HERT (Session 2)

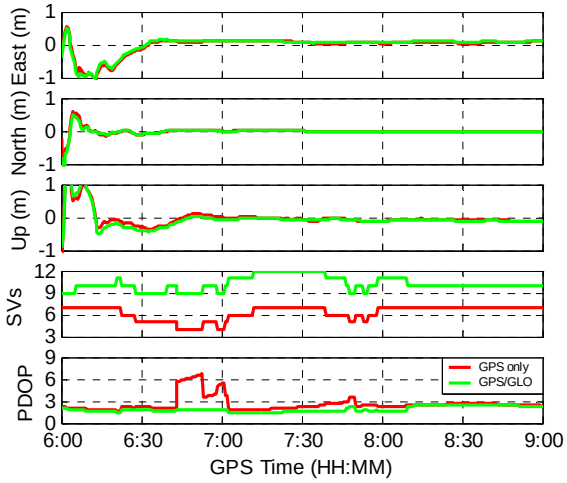


Fig. 8 Processing results at HERT (Session 3)

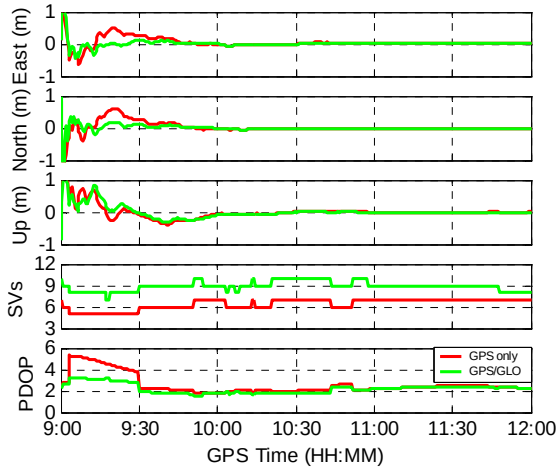


Fig. 9 Processing results at HERT (Session 4)

Table 2 shows the RMS statistics of the positioning errors at HERT station using the position results obtained from the last one and a half hours of observations from each session. A significant accuracy improvement is found in Session 2 where the improvements in the east and up components reach 4cm and 3cm respectively.

Tab. 2 RMS Statistics of Positioning Results at HERT (m)

| | | GPS Only | GPS / GLONASS |
|---|---|---|---|
| Session 1 | East | 0.101 | 0.093 |
| | North | 0.031 | 0.034 |
| | Up | 0.082 | 0.092 |
| Session 2 | East | 0.129 | 0.087 |
| | North | 0.019 | 0.018 |
| | Up | 0.060 | 0.029 |
| Session 3 | East | 0.063 | 0.085 |
| | North | 0.024 | 0.012 |
| | Up | 0.083 | 0.091 |
| Session 4 | East | 0.037 | 0.035 |
| | North | 0.012 | 0.011 |
| | Up | 0.013 | 0.013 |

Figs. 10-13 show the processing results at GOPE station. No convergence improvement is found in Fig. 10 while a slight improvement in the east component can be seen from Fig. 11. Look at Fig. 12, the convergence in the combined PPP processing appears more stable and smooth between 7:00 and 7:40 when compared to the GPS-only processing results. Fig. 13 indicates a slight improvement in the beginning of the convergence process.

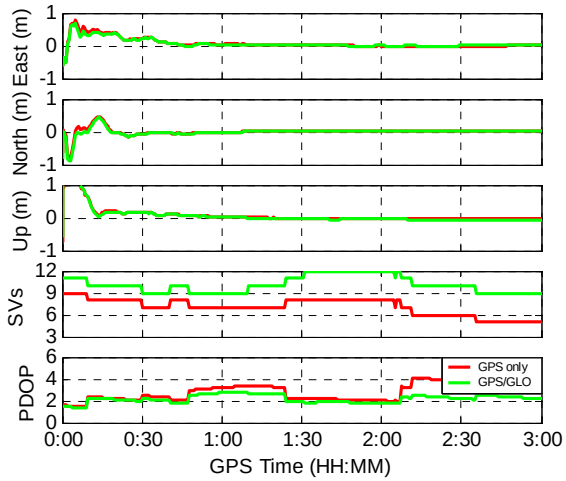


Fig. 10 Processing results at GOPE (Session 1)

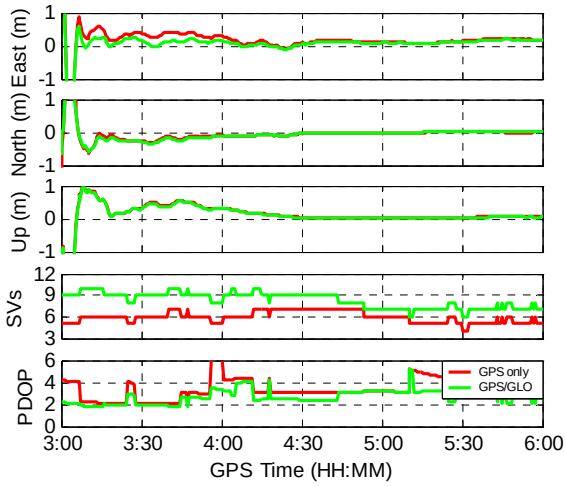


Fig. 11 Processing results at GOPE (Session 2)

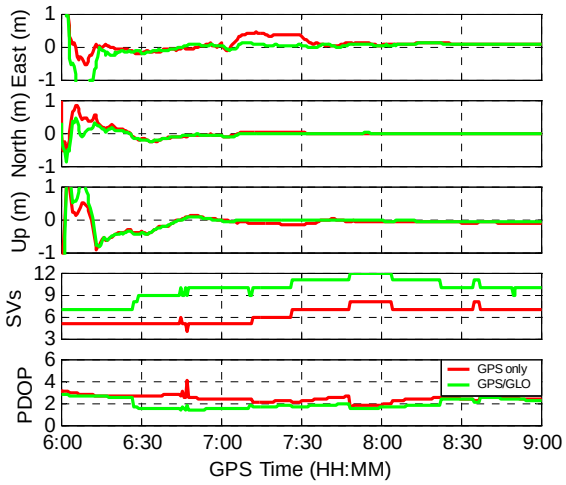


Fig. 12 Processing results at GOPE (Session 3)

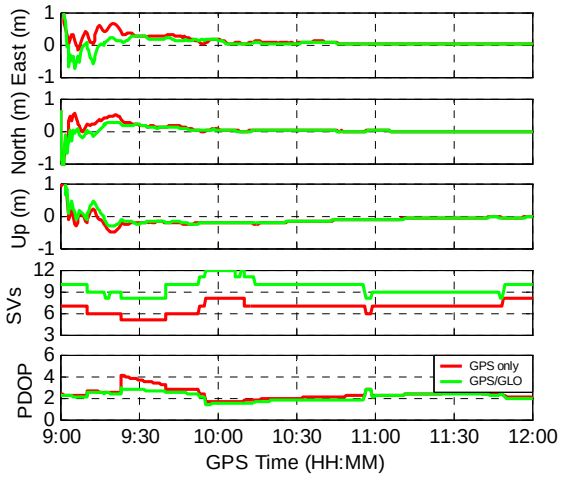


Fig. 13 Processing results at GOPE (Session 4)

Presented in Table 3 is the RMS statistics of positioning results at GOPE station. The maximum accuracy improvement is 3cm which can be seen in the east component of Session 3 while the accuracy degradation of 2cm is also found in the up component of Session 1.

Tab. 3 RMS Statistics of Positioning Results at GOPE (m)

| | | GPS Only | GPS / GLONASS |
|---|---|---|---|
| Session 1 | East | 0.008 | 0.008 |
| | North | 0.010 | 0.018 |
| | Up | 0.030 | 0.051 |
| Session 2 | East | 0.147 | 0.128 |
| | North | 0.019 | 0.017 |
| | Up | 0.044 | 0.031 |
| Session 3 | East | 0.098 | 0.069 |
| | North | 0.018 | 0.014 |
| | Up | 0.084 | 0.059 |
| Session 4 | East | 0.045 | 0.040 |
| | North | 0.010 | 0.008 |
| | Up | 0.099 | 0.098 |

The processing results at YARR station are presented in Figs. 14-17. A significant convergence improvement has been found in the east direction in Fig. 14 where observations from an average of four GLONASS satellites are utilized in the combined processing during the period of 0:00 to 1:30. No convergence improvement is found in the other figures by adding the GLONASS observations due to limited number of visible GLONASS satellites. This indicates a correlation between position convergence improvement and satellite geometry improvement. Table 4 shows the RMS statistics results of the poisoning errors at YARR station. The maximum accuracy improvement of 13cm occurs in the east direction of Session 1.

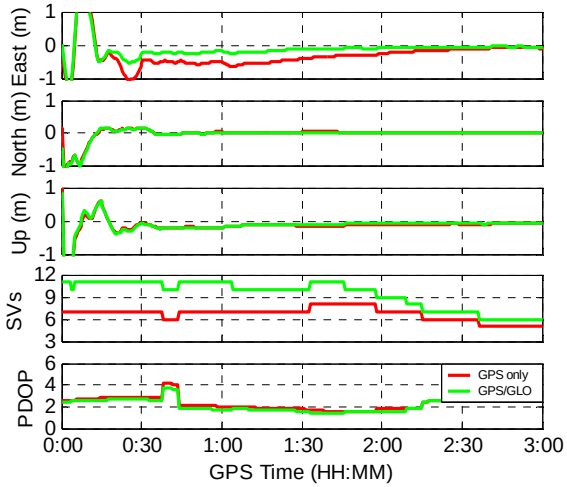


Fig. 14 Processing results at YARR (Session 1)

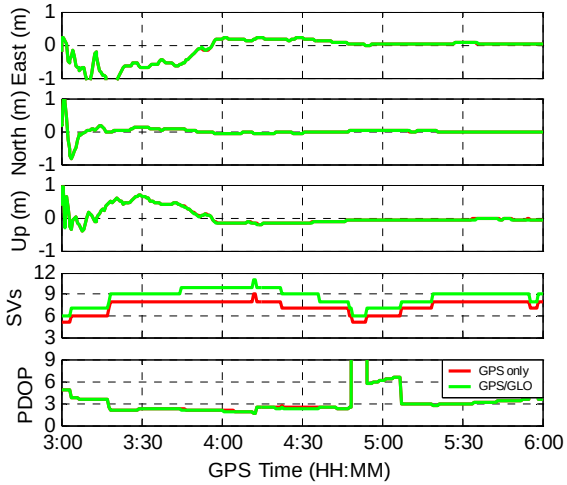


Fig. 15 Processing results at YARR (Session 2)

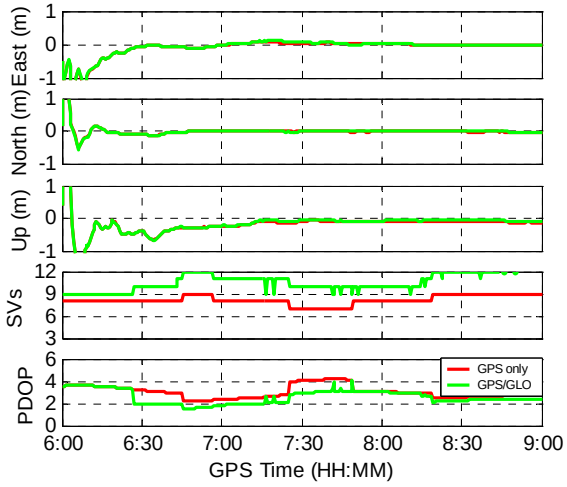


Fig. 16 Processing results at YARR (Session 3)

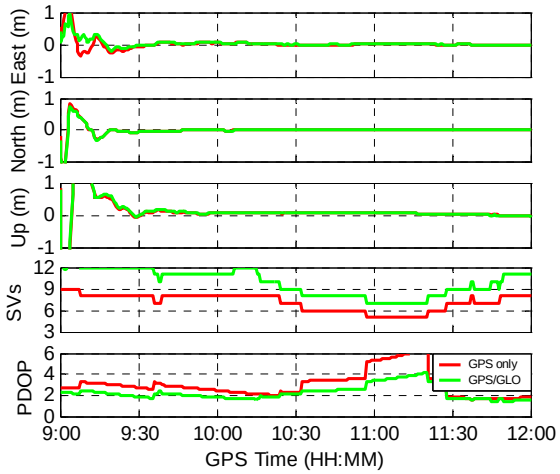


Fig. 17 Processing results at YARR (Session 4)

Tab. 4 RMS Statistics of Positioning Results at YARR (m)

| | | GPS Only | GPS / GLONASS |
|---|---|---|---|
| Session 1 | East | 0.209 | 0.074 |
| | North | 0.011 | 0.009 |
| | Up | 0.112 | 0.086 |
| Session 2 | East | 0.063 | 0.064 |
| | North | 0.016 | 0.016 |
| | Up | 0.078 | 0.080 |
| Session 3 | East | 0.021 | 0.025 |
| | North | 0.021 | 0.020 |
| | Up | 0.100 | 0.075 |
| Session 4 | East | 0.017 | 0.018 |
| | North | 0.005 | 0.005 |
| | Up | 0.047 | 0.050 |

In order to compare the positioning accuracy between using GPS-only observations and combined GPS/GLONASS observations, the positioning accuracy derived from three-dimensional coordinate component errors is presented in Fig. 18. As can be seen, the improvement of the positioning accuracy is obvious for most of the position results, and the maximum improvement reaches 12cm.

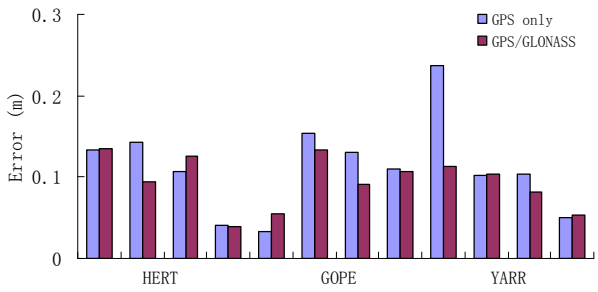


Fig. 18 Positioning accuracy comparison

## 5 CONCLUSIONS

A positioning model based on combined GPS and GLONASS observations has been proposed in this paper for precise point positioning. In order to assess the positioning accuracy and convergence time improvement of the combined GPS and GLONASS data processing, a 12-hour and four 3-hour sessions of datasets have been used in the data analysis. Comparisons have been conducted between GPS only and combined GPS/GLONASS processing. Based on the results, current GLONASS constellation has not caused a significant impact on the positioning results including position coordinates, receiver clock offset and zenith wet tropospheric delay since only two or three GLONASS satellites were observed most of time at any specific time. More significant improvements are expected when with more GLONASS satellites available in space. The research results further indicate that even with limited number of GLONASS satellites the improvement of the position convergence time is dependent on the improvement level of the satellite geometry for position determination. The results also indicate that the positioning accuracy can be improved by additional GLONASS observations in most cases. Further investigation will be conducted to assess the combined GPS/GLONASS precise point positioning in a kinematic mode.

## ACKNOWLEDGMENTS

The financial supports from NSERC and GEOIDE are greatly appreciated. The contribution of data from the International GNSS Service (IGS) and Information-Analytical Center (IAC) is also appreciated.

Based on a paper presented at The Institute of Navigation International Technical Meeting, Fort Worth, Texas, September 2007.

## REFERENCES

Bruyninx, C. (2007). ***Comparing GPS-only with GPS+GLONASS positioning in a Regional Permanent GNSS Network***. *GPS Solution*, 11:97-106, 2007.

Habrich, H. (1999). ***Geodetic Applications of the Global Navigation Satellite System (GLONASS) and of GLONASS/GPS Combinations.*** PhD Thesis, University of Berne.

Habrich, H., P. Neumaier, K. Fisch (2004). ***GLONASS Data Analysis for IGS***. Proceedings of IGS Workshop and Symposium, University of Berne, 2004.

Kaplan, E.D., C.J. Hegarty (2006). ***Understanding GPS: Principles and Applications***. 2nd Edition. Artech House.

Oleynik, E.G., V.V. Mitrikas, S.G. Revnivykh, A.I. Serdukov, E.N.Dutov, V.F.Shiriaev (2006). ***High-Accurate GLONASS Orbit and Clock Determination for the Assessment of System Performance.*** Proceedings of ION GNSS 2006, Fort Worth, TX, September 26-29, 2006.

Romero, I., J.M.Dow, R. Zandbergen, J.Feltens, C.Garcia, H.Boomkamp, J.Perez (2004), ***The ESA/ESOC IGS Analysis Center Report 2002***, IGS 2001-2002 Technical Report, 53-58, IGS Central Bureau, JPL-Publication, 2004.

Schaer, S.T., U. Hugentobler, R. Dach, M. Meindl, H. Bock, C.Urschl, G. Beutler (2004). ***GNSS Analysis at CODE.*** Proceedings of IGS Workshop and Symposium. University of Berne.

Sergey, K., R. Sergey, T. Suriya (2007). ***GLONASS as a Key Element of the Russian Positioning Service***. Advances in Space Research, 39:1539-1544.

Tsujii, T., M. Harigae, T. Inagaki, T. Kanai (2000). ***Flight Tests of GPS/GLONASS Precise Positioning versus Dual Frequency KGPS Profile***. Earth Planets Space, 52: 825-829.

Weber, R., E. Fragner (2002). ***The Quality of Precise GLONASS Ephemerides***. Adv. Space Res. 30(2), 271-279, 2002.

Weber, R., J.A. Slater, E. Fragner, V. Glotov, H. Habrich, I.Romero, S. Schaer (2005). ***Precise GLONASS Orbit Determination within the IGS/IGLOS Pilot Project***. Advances in Space Research, 36: 369-375.

Zinoviev, A.E (2005).***Using GLONASS in Combined GNSS Receivers: Current Status.*** Proceedings of ION GNSS 2005, Long Beach, CA, September 13-16, 2005.